Available online at www.sciencedirect.com
ScienceDirect
Catalysis Today 130 (2008) 69–74
CATALYSIS TODAY
www.elsevier.com/locate/cattod

New insights into the role of glycol-based additives in the improvement of hydrotreatment catalyst performances

Victor Costa [a], Karin Marchand [a], Mathieu Digne [a,*], Christophe Geantet [b]

[a] IFP, IFP-Lyon, BP 3, 69390 Vernaison, France
[b] IRCELYON, UMR-CNRS 5256, Université Claude Bernard – Lyon I, 2 avenue A. Einstein, 69626 Villeurbanne Cedex, France

Available online 2 July 2007

Abstract

The introduction of a glycol-type additive in hydrotreating catalysts is an efficient procedure to improve catalytic activity. Nevertheless, controversial explanations about the activity enhancement mechanism exist in the literature. This may be due to different catalyst preparation procedures, different location of the additive impregnation step, or simply because several phenomena are implied in this improvement. The aim of this work is thus to rationalize the roles of these additives with respect to (i) species present in the impregnation solution as well as on the catalyst surface and (ii) the preparation step where the additive impregnation is performed, i.e. after drying or after calcination. Different impregnation solutions have been used containing (a) ammonium heptamolybdate or cobaltomolybdate heteropolyanions for CoMo catalysts and (b) phosphomolybdate heteropolyanion with different P/Mo molar ratio for CoMoP catalysts. Surface species have been thoroughly characterized for dried and calcined catalysts prior to and after the additive impregnation using triethyleneglycol. For all dried and calcined CoMo and CoMoP catalysts, a redissolution phenomenon has been evidenced after the additive impregnation, leading to the formation of the Anderson heteropolyanion $AlMo_6O_{24}H_6^{3-}$. This redissolution phenomenon is however limited by the low solubility of $AlMo_6O_{24}H_6^{3-}$. Moreover, in the case of CoMoP dried catalysts (P/Mo molar ratio ≥ 0.4), characterization of additive-containing catalysts evidenced $PCoMo_{11}O_{40}^{7-}$ formation. Redissolution and redispersion due to the additives are thus enhanced because phosphomolybdic species have a much higher solubility than $AlMo_6O_{24}H_6^{3-}$. Similar observations, although less pronounced, may be drawn for calcined catalysts. Indeed, a stronger precursor–support interaction has been created during calcination. Catalysts performances were evaluated in toluene hydrogenation and activities obtained match perfectly.
© 2007 Elsevier B.V. All rights reserved.

Keywords: Hydrotreating catalyst; Additive; Glycol; Heteropolyanion; Raman spectroscopy

1. Introduction

More stringent environmental constraints lead to reduce sulfur levels in diesel fuels from 50 to 10 wppm by 2009 [1]. To produce ultra low sulfur diesel (ULSD), further activity improvements of middle distillates hydrotreating catalysts are required. Middle distillates hydrotreating (HDT) catalysts are transition metal sulfide, such as MoS_2, promoted by a group VIII metal, such as Co, and supported on a high specific surface area support, such as γ-alumina. The "CoMoS" active phase consists in well-dispersed MoS_2 nanocrystallites decorated by cobalt atoms [2–4]. This phase is obtained by sulfidation of the oxide precursors, usually deposited on the support surface by incipient wetness impregnation. Many improvements of HDT catalysts preparations have been proposed, involving a better knowledge of polyoxomolybdate solution chemistry, more insights into support–active phase interaction and new activation procedures.

One simple and efficient method to boost catalytic activity is the inclusion of an organic molecule in the catalyst preparation. For instance, glycol molecules, such as diethyleneglycol monobutyl ether (DEGbe) or triethyleneglycol (TEG), have been proposed as suitable compounds, leading to significant gains in hydrodesulfurization activity [5]. These gains are observed whenever the additive impregnation is performed: additive impregnation on support prior to active phase precursors impregnation, simultaneous impregnation of the cobalt and molybdenum precursors and the additive, post-impregnation of the additive on dried or calcined catalyst.

* Corresponding author. Tel.: +33 4 78 02 26 22; fax: +33 4 78 02 27 45.
E-mail address: mathieu.digne@ifp.fr (M. Digne).

0920-5861/$ – see front matter © 2007 Elsevier B.V. All rights reserved.
doi:10.1016/j.cattod.2007.05.013

Catalytic improvement is well established in the literature: for instance, a 20–30% increase in tetraline hydrogenation activity was obtained using commercial calcined CoMo(P) catalysts post-impregnated with DEGbe [6] as well as a 5–15% increase in thiophene HDS activity using TEG-containing catalysts coimpregnated with a CoMo(P) solution [7]. Nevertheless, the origins of the activity enhancement remain controversial. On the one hand, authors have concluded that glycol-type additives act as low temperature sulfidation inhibitors ($T < 473$ K) [6]. In contradiction, other studies reported increased low temperature sulfidation for additive-containing catalysts [7]. One possible origin of these discrepancies may come from the nature of the oxide precursors used. The conventional impregnation solution for HDT catalysts is obtained by dissolution of ammonium heptamolybdate (AHM) and cobalt nitrate. Besides that, solutions containing molybdenum heteropolyanions (HPA) are used to obtain improved catalysts: for instance, phosphomolybdate anions, such as $PMo_{12}O_{40}^{3-}$ or $P_2Mo_5O_{23}^{6-}$ [8,9], and more recently cobaltohexamolybdate Anderson HPA $CoMo_6O_{24}H_6^{3-}$ and its dimeric form, $Co_2Mo_{10}O_{38}H_4^{6-}$ [10,11] have been proposed as efficient precursors. The effect of additives may be different for each precursor, since different surface species are involved. Especially in the case of dried CoMo catalysts, the advantage of cobaltomolybdate heteropolyanions with respect to AHM and $Co(NO_3)_2$ precursors is that their sulfidation is not delayed by ammonium and nitrate presence. Another possible origin of these discrepancies may be the preparation step where the additive is introduced. One of the main role of glycol seems to be achieved during the support impregnation: glycol hinders the interaction between the active phase precursors and alumina [7]. By so doing, the additive favors the formation of oxidic clusters with a very high Co/Mo atomic ratio. As a consequence, more cobalt atoms are available to promote MoS_2 crystallites formed upon sulfidation. However, this explanation does not account for HDS improvements observed when additivation if performed on calcined catalysts such as observed elsewhere [6]. The location of the additive impregnation step (directly over the support, coimpregnation with CoMo(P) precursors, impregnation of dried or calcined catalysts) may thus imply different phenomena since surface species may be different.

The aim of the present work is thus to rationalize the influence of the additive on the catalytic performances with respect to the preparation step where the additive impregnation is performed as well as to the precursor solutions. Starting from different polyoxomolybdate precursors, catalysts were prepared and the additive impregnation was performed on dried as well as calcined catalysts. All catalysts were characterized mainly using Raman and UV–vis spectroscopies. Their catalytic activity was evaluated in toluene hydrogenation.

2. Experimental

2.1. Catalysts preparation

For all prepared CoMo(P) catalysts, the support was commercial γ-alumina extrudates (specific surface area of 300 $m^2\ g^{-1}$). The molybdenum loading was fixed at 18 wt% MoO_3. The impregnation was performed using the incipient wetness impregnation method. After 12 h of aging (room temperature, water-saturated atmosphere), the catalysts were dried at 393 K for 2 h. A fraction of the dried catalyst was calcined at 773 K for 2 h under air flow. Dried and calcined catalysts are, respectively noted (D) and (C).

Our first objective is to determine the influence of the deposited precursors nature on the additive-containing catalysts efficiency. For this purpose, catalysts were prepared from different impregnation solutions. The first impregnation solution was obtained by water dissolution of ammonium heptamolybdate (AHM) and cobalt nitrate, with a Co/Mo molar ratio of 0.4. The impregnation was performed in two steps, with an intermediate drying step. The corresponding catalyst is noted CoMo_AHM(D). The second impregnation solution contained the $Co_2Mo_{10}O_{38}H_4^{6-}$ heteropolyanion (HPA). This preparation was performed according to the procedure described in [10]. For this solution, Co ions in the HPA species exhibit a 3+ oxidation state, whereas the Co counterions exhibit a 2+ oxidation state. The Co/Mo molar ratio is 0.5 and the catalysts are noted CoMo_HPA(D). Phosphorus-containing impregnation solutions were also prepared by dissolution of molybdenum trioxide and cobalt hydroxide and addition of H_3PO_4. The Co/Mo molar ratio was fixed to 0.4 and three P/Mo molar ratio were investigated: 0.11, 0.40 and 0.57. The first one corresponds to the stoichiometry of the lacunary Keggin $PMo_9O_{34}H_4^{5-}$ HPA and the second one to the $P_2Mo_5O_{23}^{6-}$ HPA. These catalysts are noted CoMoP(*x*D), where *x* stands for the phosphorous content, expressed as P_2O_5 wt% on the catalyst. Accordingly, calcined catalysts are noted CoMo_AHM(C), CoMo_HPA(C) and CoMoP(*x*C).

Our second objective is to determine the influence of the preparation unitary step where additive impregnation is performed. The additive impregnation step was thus performed after drying or after calcination by incipient wetness impregnation of the catalyst with an aqueous solution of triethyleneglycol (TEG). The TEG concentration was fixed in order to obtain a TEG/Mo molar ratio close to 0.75. After impregnation, the catalysts were aged for 12 h at ambient temperature and dried for 6 h at 343 K and 5 kPa. No calcination was applied on additive-containing catalysts.

2.2. Sample characterization

The molybdenum, cobalt, phosphorus and aluminium loadings of the prepared catalysts (Table 1) were determined by X-ray fluorescence (Philips PW2404 spectrometer) and TEG loadings were determined using the carbon content, obtained by elemental analysis (CE Instruments EA1110). Electronic scanning microscopy was used to determine the elemental distribution profile inside the catalyst extrudates. Results are expressed by a distribution coefficient *R* averaged for 10 extrudates. This coefficient evaluates the homogeneity of an element concentration throughout the catalyst body: $R = 1$ for flat profiles, $R < 1$ for egg-shell profiles and $R > 1$ for egg-yolk profiles. Laser Raman (argon laser at 514 nm) and UV–vis

Table 1
Additive-free and additive-containing catalysts prepared and evaluated in toluene hydrogenation

Catalyst	P/Mo (molar ratio)	TEG/Mo (molar ratio)	r_{HYD} (mmol cm^{-3} h^{-1})
CoMo_AHM(D)	0	0	0.92
CoMo_AHM(D) + TEG	0	0.78	1.04
CoMo_HPA(D)	0	0	1.14
CoMo_HPA(D) + TEG	0	0.71	1.36
CoMoP(1D)	0.12	0	1.09
CoMoP(1D) + TEG	0.12	0.85	1.29
CoMoP(3D)	0.38	0	1.18
CoMoP(3D) + TEG	0.38	0.81	1.74
CoMoP(5D)	0.54	0	1.29
CoMoP(5D) + TEG	0.54	0.80	1.82
CoMo_AHM(C)	0	0	1.32
CoMo_AHM(C) + TEG	0	0.76	1.46
CoMo_HPA(C)	0	0	1.44
CoMo_HPA(C) + TEG	0	0.63	1.36
CoMoP(1C)	0.12	0	1.21
CoMoP(1C) + TEG	0.12	0.80	1.25
CoMoP(3C)	0.38	0	1.52
CoMoP(3C) + TEG	0.38	0.77	1.59
CoMoP(5C)	0.54	0	1.52
CoMoP(5C) + TEG	0.54	0.77	1.58

D stands for dried catalyst; C for calcined catalyst; _AHM for standard preparation (ammonium heptamolybdate and cobalt nitrate); _HPA for cobaltomolybdate heteropolyanions.

spectroscopies were also used as characterization methods. Raman spectra were obtained using a Jobin Yvon LabRam HR spectrometer and UV–vis spectra using a Varian Cary 4G spectrometer, equipped with a Praying Mantis (Harrick) for solid analysis.

2.3. Sulfidation and catalytic tests

Sulfidation as well as toluene hydrogenation test were conducted at 623 K and 6 MPa. The liquid feed contained 74.1 wt% cyclohexane, 20.0 wt% toluene and 5.9 wt% dimethyldisulfide, used as sulfiding agent. The H_2/feed ratio was constant and equal to 450 N l/l. The liquid feed flow was 8 cm^3 h^{-1} (LHSV of 4 h^{-1}) during the sulfidation stage and 4 cm^3 h^{-1} (LHSV of 2 h^{-1}) during the catalytic test. The oxidic catalyst was crushed and the 315–1000 μm fraction was diluted in solid SiC (6 cm^3 for 2 cm^3 of catalyst). After sulfidation (2 K min^{-1} followed by 1 h at 623 K), conversions were determined by on-line gas chromatography every hour after the first measurement. The test was 5 h long. Catalytic results were expressed in terms of toluene hydrogenation (HYD) reaction rates, calculated from the measured toluene conversions (hydrogenation products).

3. Results and discussion

3.1. Characterization of additive-free and additive-containing dried catalysts

The Raman spectra of dried catalysts CoMo_AHM(D), CoMo_HPA(D) CoMoP(1D) and CoMoP(3D) are similar

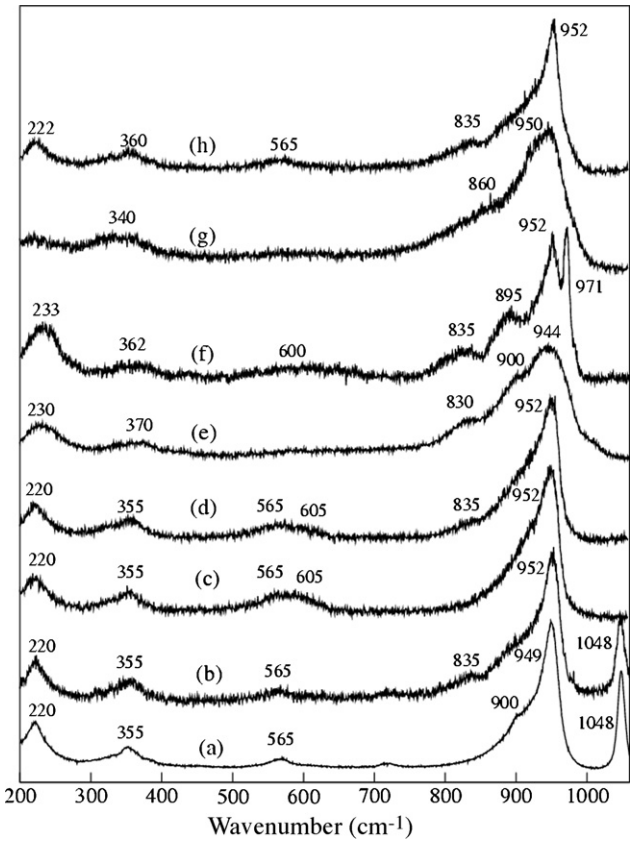

Fig. 1. Raman spectra of (a) additive-free and (b) TEG-containing CoMo_AHM(D) catalysts, (c) additive-free and (d) TEG-containing CoMo_HPA(D) catalysts, (e) additive-free and (f) TEG-containing CoMoP(5D) catalysts, (g) additive-free and (h) TEG-containing CoMo_HPA(C) catalysts.

(Fig. 1a): they exhibit bands at about 952 (intense), 900 (shoulder), 565, 355 and 220 cm^{-1}. These bands correspond to an Anderson heteropolyanion XMo_6O_{24}. For the CoMo_AHM(D), CoMoP(1D) and CoMoP(3D) catalysts (P/Mo < 0.4, corresponding to the $P_2Mo_5O_{23}^{6-}$ stoichiometry), Raman spectra demonstrate the presence of the $AlMo_6O_{24}H_6^{3-}$ species. The formation of hexamolybdoaluminate [12,13] involves molybdenum-assisted dissolution of the alumina support: aluminum cations in solution react with molybdate to form $AlMo_6O_{24}H_6^{3-}$ [13]. Since hexamolybdoaluminate cobalt and ammonium salts have low solubility (respectively 0.18 and 0.12 mol Mo l^{-1} [14,15]), they precipitate on the support surface, displacing hexamolybdoaluminate formation equilibrium towards support dissolution, even at non-aggressive pH. As a consequence, the initial species in the impregnation solution ($Mo_7O_{24}^{6-}$ for CoMo_AHM catalyst and phosphomolybdic HPA for CoMoP catalysts) are mainly disintegrated during the impregnation. For the CoMo_HPA(D) catalyst, the UV–vis spectrum reveals a band at about 610 nm, assigned to Co^{3+} and the Raman spectrum exhibits an additional shoulder at 605 cm^{-1} (Fig. 1c). The spectral features are consistent with the presence of the $Co_2Mo_{10}O_{38}H_4^{6-}$ anion and its monomeric form, $CoMo_6O_{24}H_6^{3-}$ [11]. The initial species of the impregnation solution have therefore been at least partially preserved, after the impregnation. This conclusion is also true for the

CoMoP(5D) catalyst: the Raman spectrum exhibits a main band at 944 cm^{-1}, assigned to the $P_2Mo_5O_{23}^{6-}$ species (Fig. 1e). Indeed, the phosphorus content of the impregnation solution (P/Mo = 0.54), in excess compared to the $P_2Mo_5O_{23}^{6-}$ stoichiometry, limits the disintegration of the phosphomolybdate HPA. Indeed, this disintegration begins with the reaction between phosphate groups and alumina surface, which decreases the P/Mo molar ratio of the solution within alumina pores [8,16].

After the TEG impregnation, the Raman bands of the Anderson hexamolybdoaluminate species are observed for all catalysts. For the CoMo_AHM(D) and CoMo_HPA(D), no significant modification of Raman and UV–vis spectra is observed (Fig. 1b and d), except a shoulder at about 835 cm^{-1} on the Raman spectrum, arising from C–O stretching of TEG [17]. This means that the $AlMo_6O_{24}H_6^{3-}$ anions for CoMo_AHM(D) catalyst and the $Co_2Mo_{10}O_{38}H_4^{6-}$ and $CoMo_6O_{24}H_6^{3-}$ anions for the CoMo_HPA(D) were kept on the catalyst surface after the additive introduction. For the CoMo_AHM(D) catalyst, the Raman band corresponding to the nitrate ions (1048 cm^{-1}) is kept after the additive impregnation (Fig. 1a and 1b). For the CoMoP(5D) catalyst, the additive leads to the disappearance of the $P_2Mo_5O_{23}^{6-}$ species bands, replaced by those of the $AlMo_6O_{24}H_6^{3-}$ species (Fig. 1f). Moreover, for phosphorous-containing catalysts with P/Mo molar ratio equal or superior to 0.4, additivation leads to the appearance of a band at about 971 cm^{-1}, whose intensity increases with the phosphorous content (Fig. 2a). This band corresponds to a Keggin-like HPA.

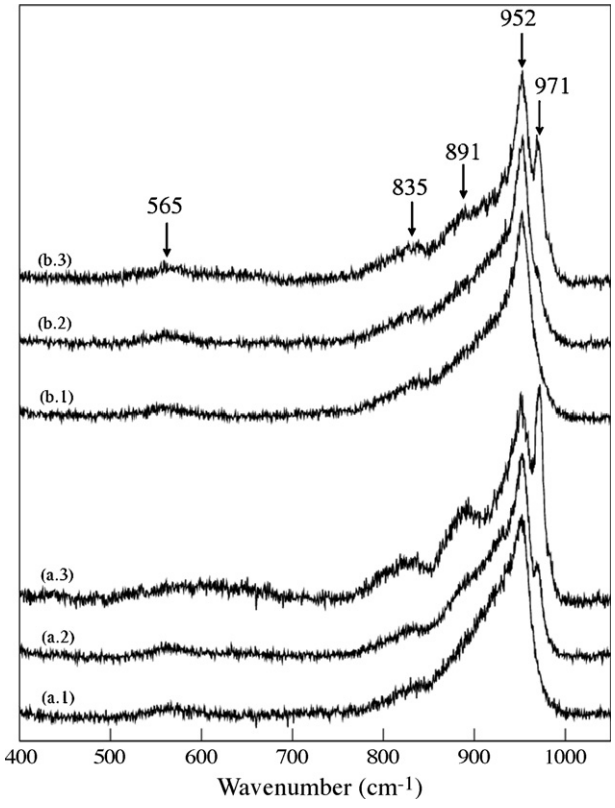

Fig. 2. Raman spectra of TEG-containing CoMoP catalysts, (a.1) CoMoP(1D), (a.2) CoMoP(3D), (a.3) CoMoP(5D), (b.1) CoMoP(1C), (b.2) CoMoP(3C) and (b.3) CoMoP(5C).

Moreover, UV–vis spectroscopy shows a band centered at about 564 nm, corresponding to a d–d transition of Co^{2+} in a distorted octahedral geometry [16]. For this reason, the Raman band at 971 cm^{-1} may be assigned to the substituted $PCoMo_{11}O_{40}^{7-}$ HPA.

As a conclusion, the presence of TEG favors surface species redissolution on dried catalysts: the Anderson $AlMo_6O_{24}H_6^{3-}$ HPA is formed in all cases and the $PCoMo_{11}O_{40}^{7-}$ HPA is also formed for phosphorous-containing catalysts with P/Mo molar ratio superior to 0.4.

3.2. Characterization of additive-free and additive-containing calcined catalysts

After calcination at 773 K, the HPA structures are destroyed for all catalysts. The Raman spectra of calcined catalysts exhibit similar features with a broad band centered at 955–950 cm^{-1} and a shoulder at about 860 cm^{-1} (Fig. 1g), corresponding to dispersed and ill-defined polyoxomolybdate structures. The existence of a $CoAl_2O_4$ phase is detected by UV–vis spectroscopy (bands at 545, 580 and 640 nm). Nevertheless, the amount of this phase seems low since the $CoAl_2O_4$ phase is not observed in XRD.

The TEG impregnation on calcined catalysts induces a similar effect than in the case of the additive impregnation on dried catalysts: the formation of the $AlMo_6O_{24}H_6^{3-}$ HPA (strong band at 952 cm^{-1} and small band at 565 cm^{-1}) is also evidenced for all catalysts (Figs. 1h and 2b). It should be noticed that, for the additive-containing CoMo_HPA(C) catalyst, the formed surface specie is now the $AlMo_6O_{24}H_6^{3-}$ HPA, instead of the $CoMo_6O_{24}H_6^{3-}$ and $Co_2Mo_{10}O_{38}H_4^{6-}$ anions as for the corresponding additive-free dried catalyst. Indeed, the shoulder at 605 cm^{-1} on the Raman spectrum is no longer observed (Fig. 1h). For catalysts with a high phosphorous content, the formation of the $PCoMo_{11}O_{40}^{7-}$ HPA (band at 971 cm^{-1}) is also observed, although less pronounced compared to dried catalysts (lower relative intensity of the Raman band). The additive impregnation has no significant effect on the $CoAl_2O_4$ phase observed by UV–vis spectroscopy.

As a consequence of this redissolution phenomenon, for P-containing catalysts, a strong impact of the additive on the phosphorus distribution over the catalyst body is evidenced by electronic scanning microscopy analysis (Table 2). Before the additive impregnation, phosphorous presents an egg-shell profile ($R < 1$) whereas cobalt and molybdenum present an uniform profile ($R = 1$). This behavior is mainly due to the reaction between free phosphates and alumina surface hydroxyls ($Al_sOH + H_2PO_4^{2-} + H^+ \rightarrow Al_sHPO_4^- + H_2O$).

Table 2
Phosphorous distribution coefficient obtained by electronic scanning microscopy for calcined CoMoP catalysts ($R = 1$ for flat distribution profiles and $R < 1$ for egg-shell distribution profiles)

Catalyst	Additive-free	H_2O-impregnated	TEG-impregnated
CoMoP(5)	0.90	–	0.94
CoMoP(3)	0.91	0.92	0.94
CoMoP(1)	0.74	0.82	0.93

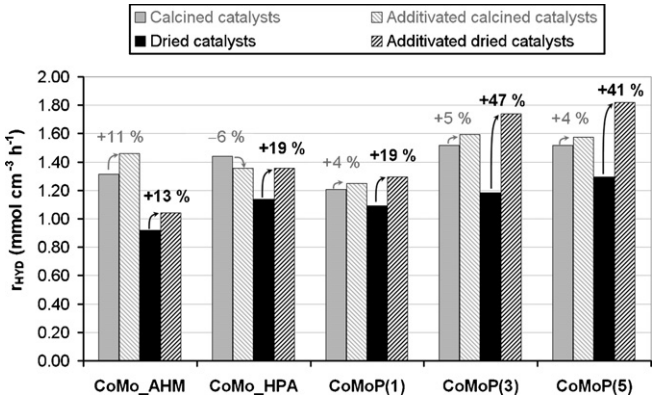

Fig. 3. Toluene hydrogenation reaction rate of as is and TEG-containing dried and calcined catalysts.

After the additive impregnation, the P profile becomes more uniform ($R = 0.93$–0.94). Such an effect is not obtained if the impregnation is only performed with water. This result shows that TEG tends to redisperse the phosphorous species over the catalyst extrudates. This redistribution is consistent with the formation of the $PCoMo_{11}O_{40}^{7-}$ HPA which has been previously evidenced. Indeed, the $PCoMo_{11}O_{40}^{7-}$ species is unstable during impregnation [16]: the reaction between free phosphates and alumina tends to decrease the P concentration and, as a consequence, $PCoMo_{11}O_{40}^{7-}$ evolves into $Mo_7O_{24}^{6-}$. The TEG diffusion into the catalyst porosity tends to release free phosphates, which react with molybdate and cobalt species to form the $PCoMo_{11}O_{40}^{7-}$ HPA.

3.3. Influence of the CoMo(P) precursors on toluene hydrogenation activity of additive-free dried and additive-containing dried catalysts

Toluene hydrogenation reaction rate expressed in toluene converted per catalyst cm^3 and per hour (mmol cm^{-3} h^{-1}) are reported in Table 1 and Fig. 3. The hydrogenation activity of the additive-free dried and the additive-containing dried CoMo_AHM catalysts are much lower than those of CoMo_HPA(D) and CoMo_HPA(D) + TEG. This is due to the fact that nitrate and ammonium, which are still present during sulfidation, are hydrogenation inhibitors. On top of that, CoMo_HPA has an improved dispersion (only one impregnation compared to CoMo_AHM catalysts prepared by two impregnations with intermediate drying) and, since cobalt and molybdenum are present within the same molecular entity, ''CoMoS'' phase formation may be favored.

The activity of CoMoP(1D) and CoMo_HPA(D) catalysts is very similar. This is expected, since $PCoMo_{11}O_{40}^{7-}$ disintegrates through phosphate reaction with alumina, leading to a decrease of the solution P/Mo molar ratio. The additive impregnation of both catalysts leads to the redissolution of the Anderson hexamolybdoaluminate heteropolyanion and accordingly, activity enhancements observed in both cases are similar (19%).

In the case of CoMoP(3D) and CoMoP(5D), a dramatic catalytic improvement (about 45%) in toluene hydrogenation is observed. This is consistent with surface species present on the additive-containing dried catalysts which both exhibit formation of $PCoMo_{11}O_{40}^{7-}$ on top of $AlMo_6O_{24}H_6^{3-}$, combined with weak precursor–support interaction (no aluminophosphates evidenced [17]).

As a conclusion, activity enhancement is closely related to surface species present on the catalyst before and after the additive impregnation. For CoMo_HPA and CoMoP(1D) catalysts, the presence of additives implies molybdenum redissolution in the form of $AlMo_6O_{24}H_6^{3-}$, but this phenomenon is limited by the low solubility of this compound in the presence of cobalt. On the other hand, for CoMoP(3D) and CoMoP(5D) catalysts (P/Mo molar ratio equal and superior to $P_2Mo_5O_{23}^{6-}$ stoichiometry), the additive impregnation leads to the molybdenum redissolution in the form of $AlMo_6O_{24}H_6^{3-}$, as well as $PCoMo_{11}O_{40}^{7-}$. Since this species has a much higher solubility, the additive induced higher activity enhancement than for the CoMo_HPA(D) and CoMoP(5D) catalysts.

3.4. Influence of the additive impregnation step location on the catalytic activity

In the case of CoMo_AHM, the additive impregnation of dried and calcined catalysts lead to the same improvement in toluene hydrogenation. However, for dried and additive-containing dried catalysts, since nitrate and ammonium are still present during sulfidation, the hydrogenation activity is inhibited compared to that of CoMo_AHM(C) and CoMo_AHM(C) + -TEG. Regarding the CoMo_HPA catalyst, TEG impregnation leads to an increase of 19% when it is performed on dried catalyst, whereas the impact becomes slightly negative on the calcined catalyst (−6%). After calcination, the cobaltomolybdate heteropolyanions are decomposed, as our Raman study evidenced. In this case, the additive impregnation allows molybdenum redispersion, via the $AlMo_6O_{24}H_6^{3-}$ formation, but the close vicinity between Co and Mo, inherited from the cobaltomolybdate heteropolyanions, is degraded. As a consequence, the beneficial effect of these starting HPA precursors is partially lost, leading to lower activity.

In the case of CoMoP catalysts, the additive impregnation of calcined catalysts leads to low activity improvements, around 5%, regardless of phosphorous content. Surface species present in all cases include hexamolybdoaluminate (Fig. 2), but its redissolution is limited by its poor solubility. Strong precursor–support interactions, especially the formation of aluminophosphate phases created during calcination [18], may limit the formation of $PCoMo_{11}O_{40}^{7-}$ in the case of CoMoP(3C), since the heteropolyanion formation is clearly evidenced on the additive-containing CoMoP(3D) catalyst. Similar arguments are also true for the CoMoP(5C) catalyst: the $PCoMo_{11}O_{40}^{7-}$ formation is observed, but less favored than the case of the CoMoP(5D) catalyst.

To conclude, catalytic improvements are related to surface species present on the catalyst surface after the additive impregnation. Calcination leads to stronger precursor–support interactions and prevents species redissolution after the additive

impregnation (low phosphorous availability). Therefore, catalytic improvements are less important in the case of the additive-containing calcined catalysts than in the case of the additive-containing dried catalysts.

4. Conclusion

The aim of this work was to rationalize the roles of glycol-based additives in HDT catalyst activity enhancement with respect to (i) species present in the impregnation solution as well as on the catalyst surface and (ii) the preparation step where the additive impregnation is performed, i.e. after drying or after calcination. Different impregnation solutions have been used containing (a) ammonium heptamolybdate or cobaltomolybdate heteropolyanions ($CoMo_6O_{24}H_7^{3-}$ and its dimeric form $Co_2Mo_{10}O_{38}H_4^{6-}$) for CoMo catalysts and (b) phosphomolybdate heteropolyanion with different P/Mo molar ratio (0.11, 0.40 and 0.57) for CoMoP catalysts. Surface species have been thoroughly characterized for all dried and calcined catalysts, prior to and after TEG impregnation. For all dried, as well as calcined CoMo and CoMoP catalysts (P/Mo molar ratio lower than 0.4), a redissolution phenomenon was evidenced after the additive impregnation step, leading to the formation of the Anderson heteropolyanion $AlMo_6O_{24}H_6^{3-}$. This redissolution phenomenon is however limited by the low solubility of this Anderson HPA. In the case of CoMoP dried catalysts (P/Mo molar ratio greater than 0.4), characterization of additive-containing catalysts evidenced $PCoMo_{11}O_{40}^{7-}$, on top of $AlMo_6O_{24}H_6^{3-}$ formation. Redissolution and redispersion due to the additive impregnation are thus enhanced because phosphomolybdic species have a much higher solubility than $AlMo_6O_{24}H_6^{3-}$. Similar, although less pronounced observations may be drawn for calcined catalysts. This may be due to the fact that stronger precursor–support interactions (aluminophosphate formation) have been created during calcination, which limit the amount of phosphates available for $PCoMo_{11}O_{40}^{7-}$ formation.

Catalysts performances, evaluated in toluene hydrogenation, are governed by surface species and thus by this redissolution–redispersion phenomenon, especially pronounced when free phosphate is available. Furthermore, such conclusions provide guidelines for a more rational additive impregnation of HDT catalysts.

Acknowledgments

We wish to thank our colleagues S. Aubineau, L. Sorbier, and especially S. Rebours for their contribution to this work.

References

[1] EU Directive 2003/17/CE 2.
[2] H. Topsøe, N.Y. Topsøe, J. Catal. 84 (1983) 386.
[3] S. Eijsbouts, Appl. Catal. A 158 (1997) 53.
[4] R.R. Chianelli, M.H. Siadati, M. Perez De la Rosa, G. Berhault, J.P. Wilcoxon, R. Bearden Jr., B.L. Abrams, Catal. Rev. Sci. Eng. 48 (2006) 1.
[5] Patent EP0601722A1 (1994).
[6] P. Mazoyer-Galliou, C. Geantet, F. Diehl, C. Pichon, T.S. Nguyen, M. Lacroix, Oil & Gas Sci. Technol. - Rev. IFP 60 (2005) 79.
[7] D. Nicosia, R. Prins, J. Catal. 229 (2005) 424.
[8] W.-C. Cheng, N.P. Luthra, J. Catal. 109 (1988) 163.
[9] A. Griboval, P. Blanchard, E. Payen, M. Fournier, J.L. Dubois, Catal. Today 45 (1998) 277.
[10] C. Martin, C. Lamonier, M. Fournier, O. Mentré, V. Harlé, D. Guillaume, E. Payen, Chem. Mater. 17 (2005) 4438.
[11] C. Lamonier, C. Martin, J. Mazurelle, V. Harlé, D. Guillaume, E. Payen, Appl. Catal. B 70 (2007) 548.
[12] L. Le Bihan, P. Blanchard, M. Fournier, J. Grimblot, E. Payen, J. Chem. Soc., Faraday Trans. 94 (1998) 937.
[13] X. Carrier, J.F. Lambert, M. Che, J. Am. Chem. Soc. 119 (1997) 10137.
[14] C.I. Cabello, I.L. Botto, H.J. Thomas, Appl. Catal. A 197 (2000) 79.
[15] C. Martin, C. Lamonier, M. Fournier, O. Mentré, V. Harlé, D. Guillaume, E. Payen, Inorg. Chem. 43 (2004) 4636.
[16] J.A. Bergwerff, L.G.A. van de Water, T. Visser, P. de Peinder, B.R.G. Leliveld, K.P. de Jong, B.M. Weckhuysen, Chem. Eur. J. 11 (2005) 4591.
[17] D. Nicosia, R. Prins, J. Catal. 234 (2005) 414.
[18] H. Kraus, R. Prins, J. Catal. 164 (1996) 251.